Imaging of Laser–Plasma X-Ray Emission with Charge-Injection Devices (CID's)

Introduction

X-ray imaging and x-ray spectroscopy are used in laser–plasma-generated physics research to diagnose conditions in the laser targets. Examples of techniques used to image x-ray emission are pinhole cameras, Kirkpatrick–Baez (KB) microscopes, curved crystal optics, and Wölter microscopes.[1–3] All spectroscopic diagnostics rely also on spatial resolution to record an x-ray spectrum. Examples of spectroscopic techniques are Bragg crystal diffraction and grating diffraction. The simplest method of recording images is time-integrated exposure of film, a common example being the calibrated Kodak direct exposure film (DEF).[4] Alternatively, images can be recorded by a solid-state device that is either directly sensitive to x rays (photons absorbed in the device) or indirectly sensitive (photons absorbed in a phosphor coating, generating visible range photons that are then absorbed in the device).

This work details the method of obtaining time-integrated images of laser–plasma x-ray emission using charge-injection devices (CID's), as has been demonstrated on the University of Rochester's 60-beam UV OMEGA laser facility.[5] The CID has an architecture similar to a charge-coupled device (CCD). The differences make them more resistant to radiation damage and, therefore, more appropriate for some applications in laser–plasma x-ray imaging. Images were obtained with pinhole cameras, KB microscopes,[2] and a tunable monochromatic x-ray microscope.[6] Simultaneous images obtained on these systems with calibrated x-ray film have enabled determination of the absolute detection efficiency of the CID's in the energy range from 2 to 8 keV.

Charge-Injection Devices (CID's)

The CID cameras used in this work are manufactured by CID Technologies, Inc. of Liverpool, NY.[7] The model CID4150 is an 812 × 604 array having square pixels with 38.5-μm center-to-center spacing and overall array dimensions of 31.3 × 23.2 mm. Details of the pixel architecture found in the literature[8–11] are summarized as follows: Each pixel contains two storage areas (pads). At the start of integration, voltage applied to both pads injects any stored charge into the substrate layer. Next, charge is accumulated under a negatively biased column storage pad until the bias is changed to transfer the stored charge to a row pad. The row pad is attached to a row preamplifier from which the signal is output and digitized. The CID's used in this work were operated at room temperature and with no conversion phosphor coating on the detector surface (direct x-ray detection). A PC-based analog-to-digital converter with 16-bit resolution, operating at 500 kHz, accomplished the camera readout. The relatively high-speed readout was employed to minimize dark current in the uncooled detectors.

Figure 83.1 shows a CID camera in its housing and an epoxy-encased dental imaging version,[11] for comparison, alongside a film pack and film pack positioner, illustrating the relative compactness of the CID camera. All signal amplification and switching electronics are contained in the CID camera. An overview of the installation on the OMEGA target chamber and surrounding structure is shown in Fig. 83.2. The

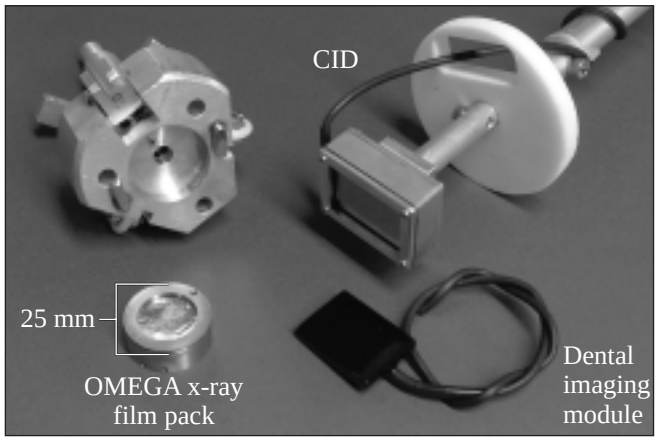

E10257

Figure 83.1
Picture of CID camera mounted on the end of a pinhole camera positioner. The CID camera replaces the film pack holder (upper left) and film pack (lower left). The CID camera was designed to be compact, as evidenced by the dental imaging version (lower right).

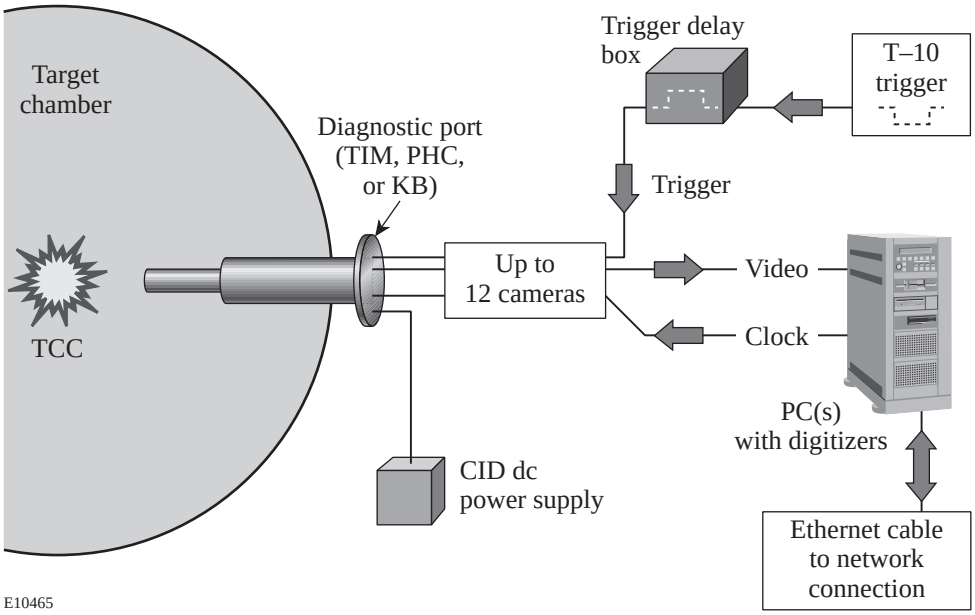

Figure 83.2
Schematic of the CID camera interface to an OMEGA x-ray diagnostic.

dc power is supplied along with a clocking line and an integration trigger line. The common integration trigger supplies each camera in use with a pre-shot pulse to acquire a background image and an on-shot pulse to acquire an image on the laser target shot. The two images are subtracted to provide the final image. The single output line contains the unformatted video signal, which is sent to a PC-based analog-to-digital converter card (ADC). Up to two PC's are used to acquire six CID camera outputs per PC, on as many as 12 CID cameras for the currently planned system.

Experiments

The CID cameras were used to obtain images of laser–plasma x-ray emission on OMEGA. Three different diagnostics were used as platforms for these tests: x-ray pinhole cameras and two different KB microscopes. One microscope was outfitted with a grating and used to obtain grating-dispersed images of target implosion cores.[12] The other microscope was outfitted with metal multilayer monochromators and used to obtain narrow-energy-band (monochromatic) x-ray images of target implosion cores.[6]

Figure 83.3 shows two images obtained with pinhole cameras located on opposite sides of the target chamber. The pinhole cameras have 11-μm pinholes and were located 170 mm from the target. The CID's were located to provide images with a magnification of 4.0 (~10 μm/pixel at the target plane). The images are of x-ray emission from a 4-mm-diam, Au-coated plastic sphere. The OMEGA beams were surface focused onto the target using the standard OMEGA optics and distributed phase plates designed to produce Gaussian-like focal spots with a diameter of ~900 μm (containing 95% of the energy). These produce x-ray spots with diameters of ~600-μm full width at half-maximum (FWHM). The images are analyzed to determine the relative pointing of each beam compared to the desired pointing (all beams pointed so as to converge at the target center, in the spherical-implosion-pointing mode). Typically six or more film-based cameras are used to obtain like images, necessitating film loading, unloading, developing, drying, and finally digitizing. Although these processes are streamlined by using auto film developers, quick drying, and video camera digitizing, the typical minimum processing time of ~40 min cannot compete with the several-minute time scale required to store and redisplay multiple digital image files.

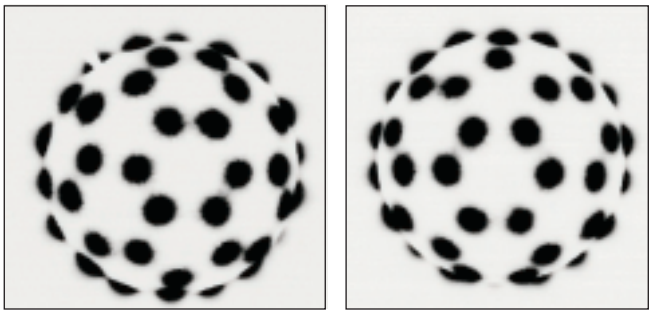

Figure 83.3
CID images taken from two opposing pinhole cameras on an OMEGA pointing shot.

Another example of CID-camera-obtained x-ray images is shown in Fig. 83.4. The CID's were located behind the same pinhole cameras described above, but farther away at a magnification of 8.0. The images are of the time-integrated x-ray emission from an imploded laser fusion target (in this case, a 3-atm-D_2-filled, 20-μm-thick CH shell). Figure 83.4(a) was taken with minimum filtration in front of the CID sensor (150 μm of Be, mostly in the pinhole camera itself), while Fig. 83.4(b) was taken with a CID on a pinhole camera on the opposite side of the target chamber and additional filtration of 50 μm of Al was used to limit the soft x-ray component of the image. Figure 83.4(a) clearly shows the target's outer-shell emission plus stalk emission (all of which occurs during target acceleration). Figure 83.4(b) shows only the harder x-ray emission that is confined to the high-density, high-temperature implosion core region.

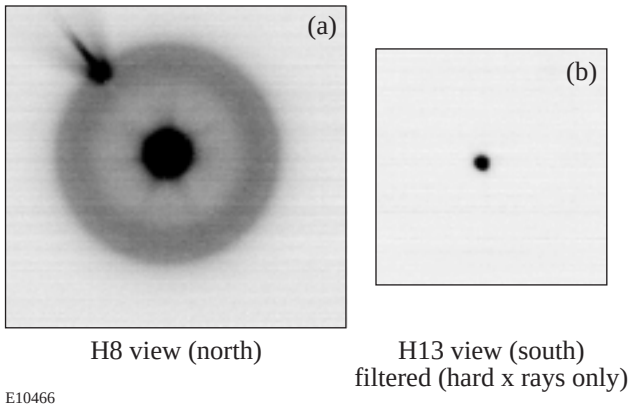

Figure 83.4
CID images of a directly driven imploding OMEGA laser target (from opposing pinhole cameras): (a) soft x-ray image containing emission from the outer shell region, the stalk, and a saturated core region; (b) hard x-ray image containing only emission from the core.

Pairs of images, one on film and one with a CID on the same x-ray microscope, have been obtained on a series of OMEGA target shots. The KB microscope was outfitted with a diffraction grating that yielded dispersed spectra of the implosion cores.[12] The magnification of the images is 20.3. Since the KB microscope is a four-mirror, four-image version with image views separated by 1.4° on the target chamber sphere, the images are nearly identical except for differences in the recording media. Figure 83.5 shows a pair of such images: (a) a film-recorded image (Kodak DEF) and (b) a CID-camera-recorded image. Both images are produced by the KB microscope, which has Ir-coated mirrors operating at grazing angles of 0.70°. Attenuation by 140 μm of Be is common to both, as is diffraction by the 0.2-μm-period transmission grating. The CID camera had an additional 25 μm of Be acting as a light shield and housing cover. Both images show nearly identical features. The main features captured by the grating-dispersed microscope (zeroth-order image of implosion and first-order diffracted image of the core) are seen in both images. Since the film and microscope have been absolutely calibrated, comparison of the film- and CID-recorded core spectra can be used to infer the absolute sensitivity of the CID pixels. Figure 83.6(a) shows such a comparison taken along the core spectrum and plotted as a function of photon energy. The CID pixel's inferred quantum efficiency dependence on energy is shown in Fig. 83.6(b). Although a precise model for the CID pixels has not been developed, the results of Janesick *et al.*[13] for the case of a front-side-illuminated, thin-depletion-region CCD are shown for comparison in Fig. 83.6(b). This model should be representative of the CID sensitivity.

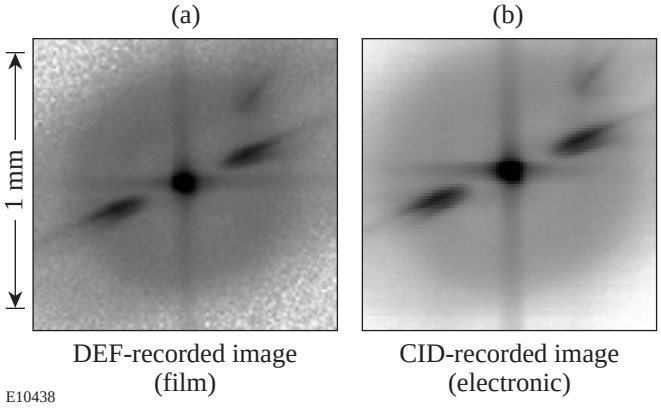

Figure 83.5
A pair of simultaneously recorded x-ray microscope images taken with (a) Kodak DEF film and (b) a CID camera. The image is an imploding OMEGA target with dispersion of the core emission by an x-ray transmission grating (evidenced by the features ~30° from the horizontal to the upper right and lower left). The horizontal and vertical streaks are due to small-angle specular scattering from the microscope mirrors.

Lastly, a pair of images taken with the KB microscope outfitted with metal multilayer monochromators is shown in Fig. 83.7. The imaging system has been previously described.[4] WB_4C multilayers with a 2d spacing of 26.5 Å were used, and the magnification of the images is 13.6. The monochromators were tuned so as to produce images of target emission centered on the Ar He-like β-line (3.683±0.011 keV) and the Ar H-like

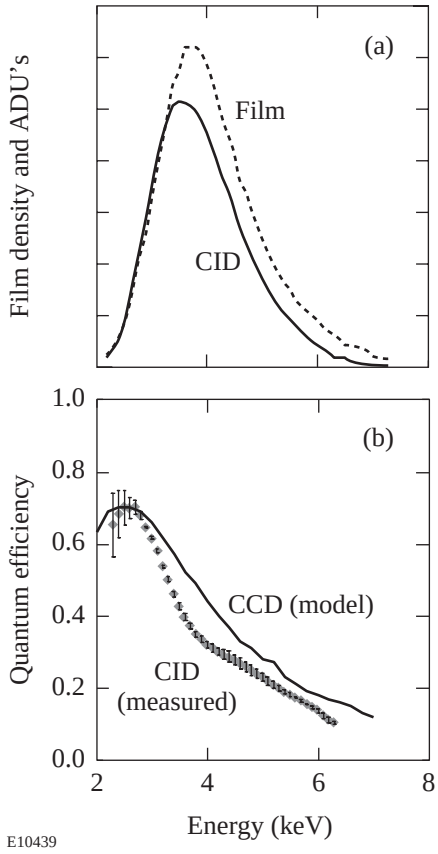

Figure 83.6
Comparison of CID- and film-recorded spectra. (a) Lineouts through the two spectral features; (b) inferred CID quantum efficiency, derived from the calibrated constants of the microscope/grating/film system.

β-line (3.935±0.012 keV), where the indicated energy range is determined by the FWHM's of the monochromator diffraction peaks. The target was a 15-atm, D_2-filled, 20-μm-thick, 1-mm-diam CH shell containing 0.35% by atomic number of Ar gas as a dopant. The images show the enhanced line-plus-continuum emission from the implosion core region. The asymmetry of the core is ascribed to the lack of perfect direct-drive beam balance on this shot, aggravated by several lower-intensity beams being near each other on the target chamber sphere. The images show a clear core region whose size and morphology can be easily measured.

Conclusion

CID cameras have been used to obtain time-integrated x-ray images on a variety of imaging and spectroscopic diagnostics on the OMEGA laser facility's target chamber. Cross calibration of the CID camera with film shows that the CID pixels, when used in direct-detection mode (i.e., without a phosphor), have a useful energy range of better than 2 to 8 keV, with additional sensitivity to be expected, especially at higher energies. Currently, all existing OMEGA time-integrated x-ray diagnostics are being outfitted with CID cameras as an optional recording medium.

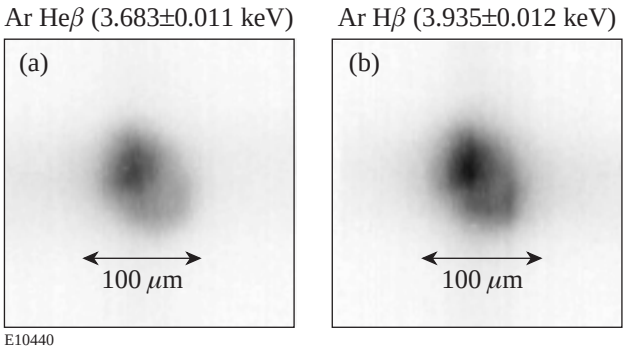

Figure 83.7
Monochromatic images of an imploding OMEGA laser target taken with two CID cameras. (a) Image of emission at 3.683±0.011 keV, centered on the Ar He-like β-line; (b) image of emission at 3.935±0.012 keV, centered on the Ar H-like β-line.

ACKNOWLEDGMENT

The authors acknowledge the support of the OMEGA laser operations group and the staff at the University of Rochester's Laboratory for Laser Energetics. This work was supported by the U. S. Department of Energy Office of Inertial Confinement Fusion under Cooperative Agreement No. DE-FC03-92SF19460, the University of Rochester, and the New York State Energy Research and Development Authority. The support of DOE does not constitute an endorsement by DOE of the views expressed in this article.

REFERENCES

1. J. A. Koch *et al.*, Appl. Opt. **37**, 1784 (1998).
2. F. J. Marshall and Q. Su, Rev. Sci. Instrum. **66**, 725 (1995).
3. N. M. Ceglio, A. M. Hawryluk, and R. H. Price, Appl. Opt. **21**, 3953 (1982).
4. B. L. Henke *et al.*, J. Opt. Soc. Am. B **3**, 1540 (1986).
5. T. R. Boehly, D. L. Brown, R. S. Craxton, R. L. Keck, J. P. Knauer, J. H. Kelly, T. J. Kessler, S. A. Kumpan, S. J. Loucks, S. A. Letzring, F. J. Marshall, R. L. McCrory, S. F. B. Morse, W. Seka, J. M. Soures, and C. P. Verdon, Opt. Commun. **133**, 495 (1997).
6. F. J. Marshall and J. A. Oertel, Rev. Sci. Instrum. **68**, 735 (1997).
7. CID Technologies, Inc., Liverpool, NY 13088.

8. Z. Ninkov, C. Tang, and R. L. Easton, in *Charge-Coupled Devices and Solid State Optical Sensors IV*, edited by M. M. Blouke (SPIE, Bellingham, WA, 1994), Vol. 2172, pp. 180–186.

9. J. J. Zarnowski *et al.*, in *Charge-Coupled Devices and Solid State Optical Sensors IV*, edited by M. M. Blouke (SPIE, Bellingham, WA, 1994), Vol. 2172, pp. 187–198.

10. J. Carbone *et al.*, in *Solid State Arrays and CCD Cameras*, edited by C. N. Anagnostoupoulos, M. M. Blouke, and M. P. Lesser (SPIE, Bellingham, WA, 1996), Vol. 2654, pp. 131–138.

11. J. Carbone *et al.*, in *Solid State Sensor Arrays: Development and Applications II*, edited by M. M. Blouke (SPIE, Bellingham, WA, 1998), Vol. 3301, pp. 90–99.

12. F. J. Marshall, J. A. Delettrez, R. Epstein, and B. Yaakobi, Phys. Rev. E **49**, 4381 (1994).

13. J. R. Janesick *et al.*, Opt. Eng. **26**, 156 (1987).